WCRP Open Science Conference: Climate Research in Service to Society, 24–28 October 2011, Denver, Colorado, U.S.A.

Coupling coefficients around the mid-latitude SST fronts in a coupled atmosphere–ocean and a stand-alone atmospheric GCMs

Nobumasa Komori,[1✉] Bunmei Taguchi,[1] Akira Kuwano-Yoshida,[1] Masami Nonaka,[2] Koutarou Takaya,[2] Wataru Ohfuchi,[1] and Hisashi Nakamura [2,3]

[1] **Earth Simulator Center**, Japan Agency for Marine-Earth Science and Technology, Yokohama, Japan
[2] Research Institute for Global Change, Japan Agency for Marine-Earth Science and Technology, Yokohama, Japan
[3] Research Center for Advanced Science and Technology, University of Tokyo, Tokyo, Japan

✉ **E-mail: komori@jamstec.go.jp**
http://www.jamstec.go.jp/esc/research/AtmOcn/

1. Introduction

Recent high-resolution satellite observation have revealed positive correlation between spatially high-pass filtered surface winds and sea surface temperature (SST) around the SST fronts, indicating that the ocean affects the atmosphere at small scales. It has been also found that divergence (curl) of wind stress correlates with downwind (crosswind) SST gradient as expected from the surface wind–SST relationship. Their regression coefficients are often regarded as a measure of the strength of their coupling and called "coupling coefficients." In this study, coupling coefficients as simulated in a coupled atmosphere–ocean and a stand-alone atmospheric general circulation models (**CFES** and **AFES**, respectively) are examined.

2. Data and Method

High-resolution simulations using **CFES** and **AFES** are conducted more than 20 years with their horizontal resolution of T239 (~50 km). The oceanic component of **CFES** has a resolution of 1/4° (~25 km) and is coupled with the atmospheric component every 20 minutes, and **AFES** is driven by daily OISST with a resolution of 1/4° based on AVHRR observation.

To examine its spatial distributions, we calculate local coupling coefficients at each grid point rather than area-averaged ones often focused in the previous studies.

3. Results

3.1. Climatology of Large-Scale Fields

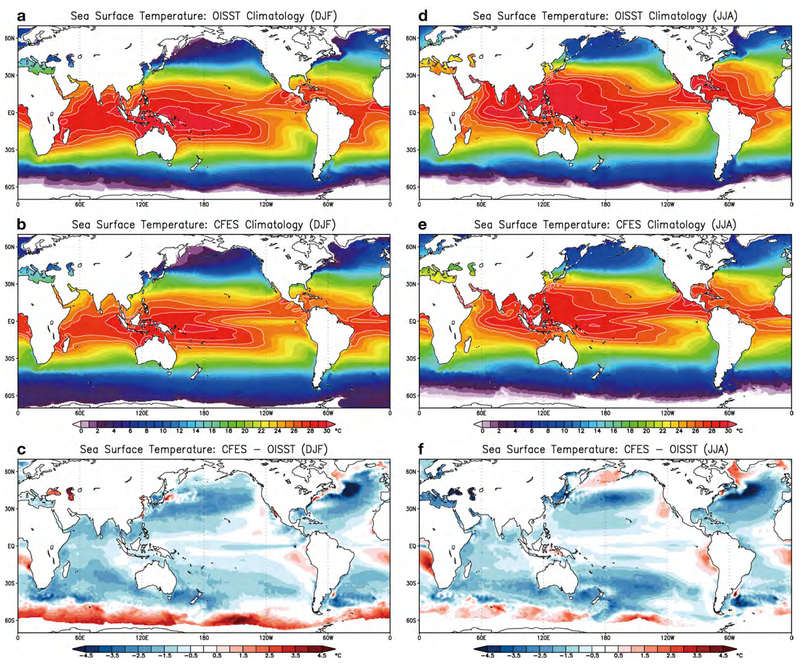

Figure 1. Climatology of SST [ºC] calculated from (top) OISST and (middle) CFES, and (bottom) their differences (CFES – OISST) for (left) DJF and (right) JJA.

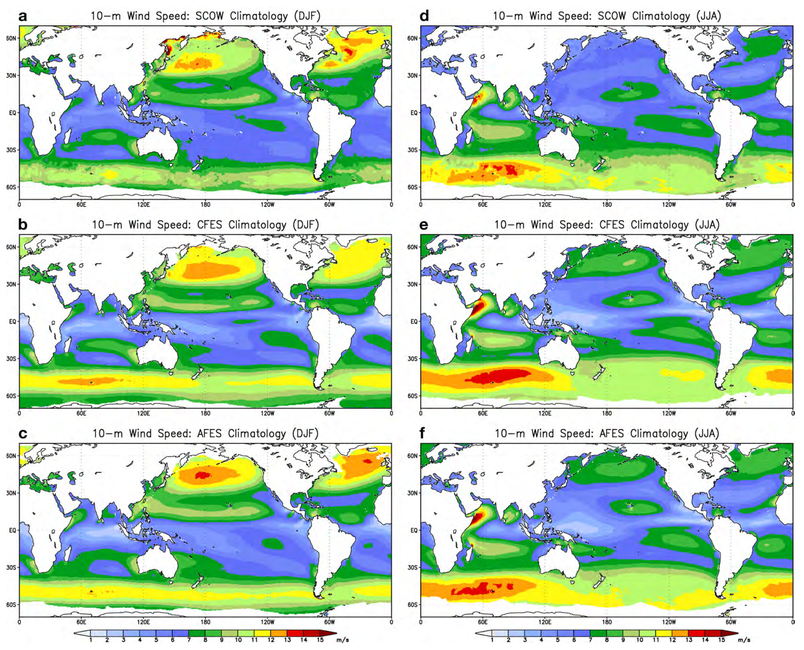

Figure 2. Climatology of 10-m wind speed [m s^{-1}] calculated from (top) SCOW [Scatterometer Climatology of Ocean Winds], (middle) CFES, and (bottom) AFES for (left) DJF and (right) JJA.

3.2. High-Pass Filtered Wind Stress Derivatives

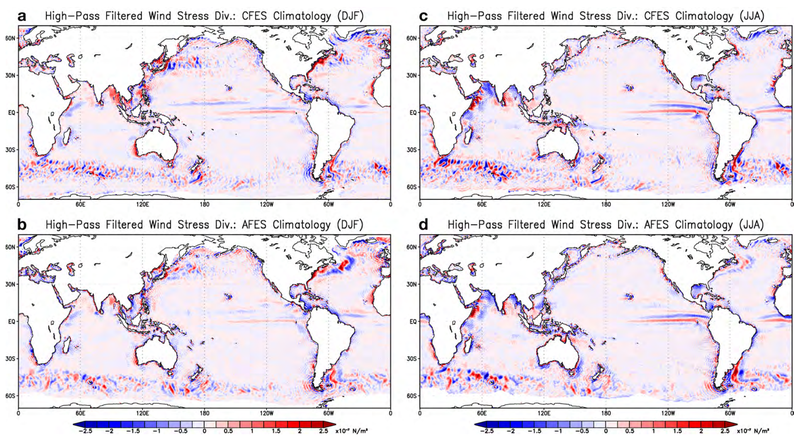

Figure 3. Climatology of high-pass filtered wind stress divergence [10^{-7} N m^{-3}] calculated from (top) CFES and (bottom) AFES for (left) DJF and (right) JJA.

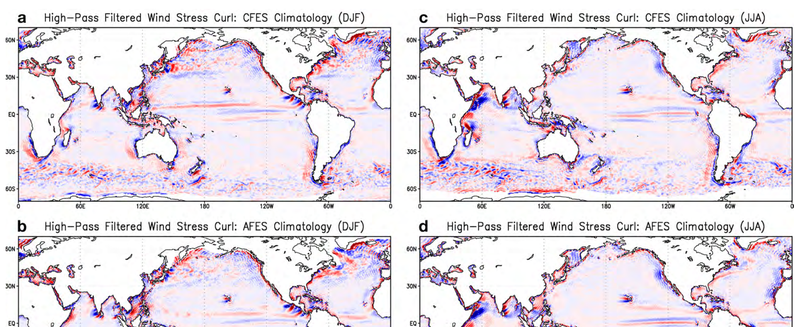

Figure 4. Same as in Fig. 3 but for high-pass filtered wind stress curl [10^{-7} N m^{-3}].

3.3. Coupling Coefficients

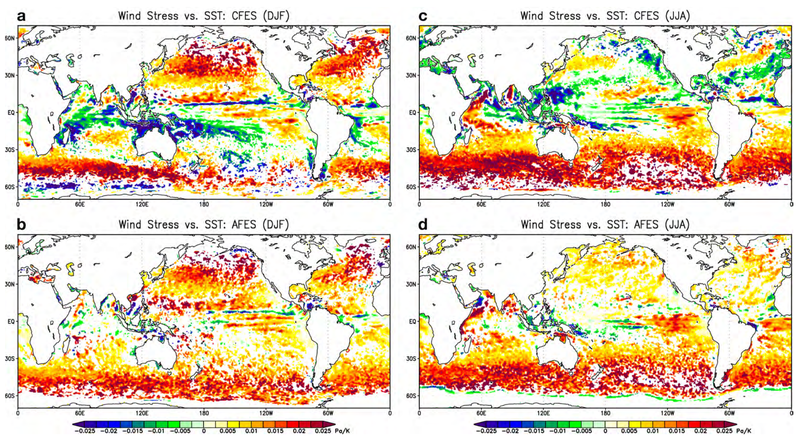

Figure 5. Coupling coefficient between SST and wind stress [Pa K^{-1}] calculated from (top) CFES and (bottom) AFES for (left) DJF and (right) JJA. Sea-ice regions are masked out.

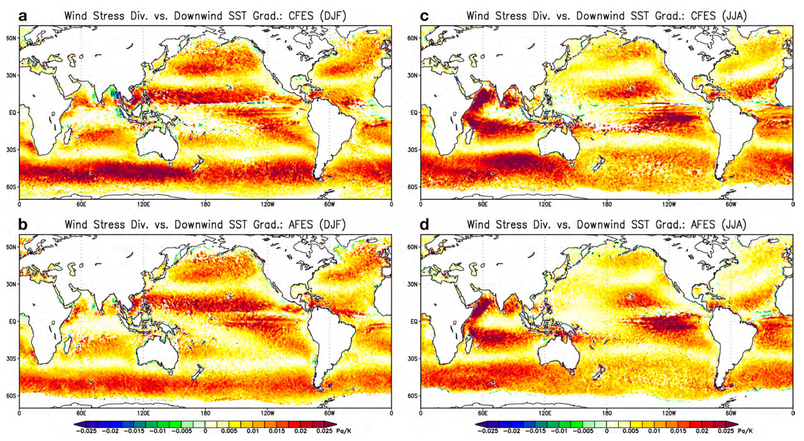

Figure 6. Same as in Fig. 5 but for coupling coefficient between downwind SST gradient and wind stress divergence [Pa K^{-1}].

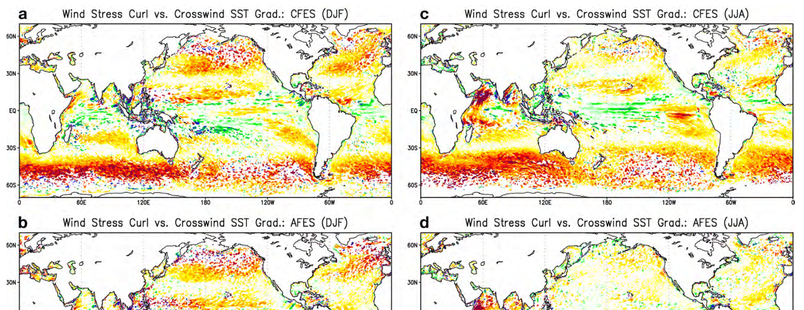

Figure 7. Same as in Fig. 5 but for coupling coefficient between crosswind SST gradient and wind stress curl [Pa K^{-1}].

Figure 8. Same as in Fig. 5 but for coupling coefficient between SLP Laplacian and wind stress divergence [m].

While wind stress positively correlates with SST only around the SST fronts such as the mid-latitude western boundary current (WBC) regions in **CFES**, both **CFES** and **AFES** well reproduced positive correlation between wind stress derivatives and SST gradients all over the world ocean. It is found that coupling coefficients between wind stress derivatives and SST gradients do not have their maxima over the WBCs including the Agulhas Return Current and their spatial patterns strongly reflect large-scale wind field in both **CFES** and **AFES**. While previous studies have focused on static stability effects on spatial and seasonal variability of area-averaged coupling coefficients, this study suggests that the variability of the coupling coefficients can also be attributed to large-scale variability of wind, and we need to distinguish between the contributions to coupling coefficients from the local efficiency of vertical momentum transfer and those from the large-scale available momentum.

3.4. Agulhas Return Current Region

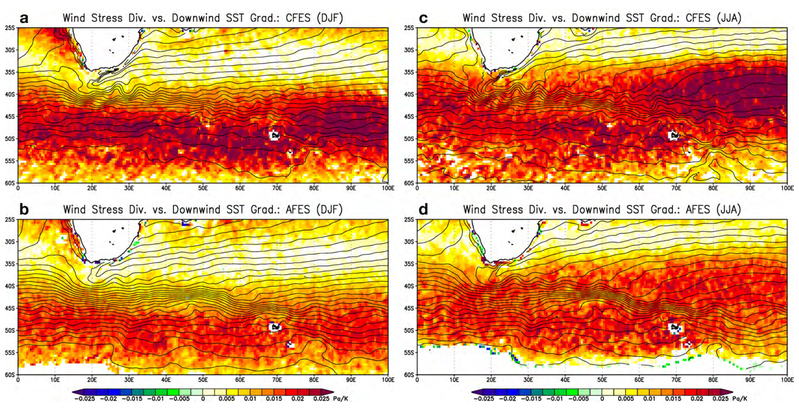

Figure 9. Coupling coefficient between downwind SST gradient and wind stress divergence [Pa K^{-1}]. Climatology of SST is also plotted in coutours and the interval is 1 K.

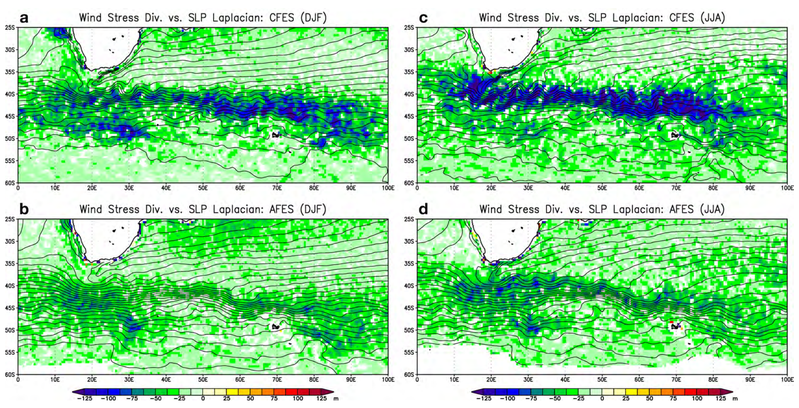

Figure 10. Same as in Fig. 9 but for coupling coefficient between SLP Laplacian and wind stress divergence [m].

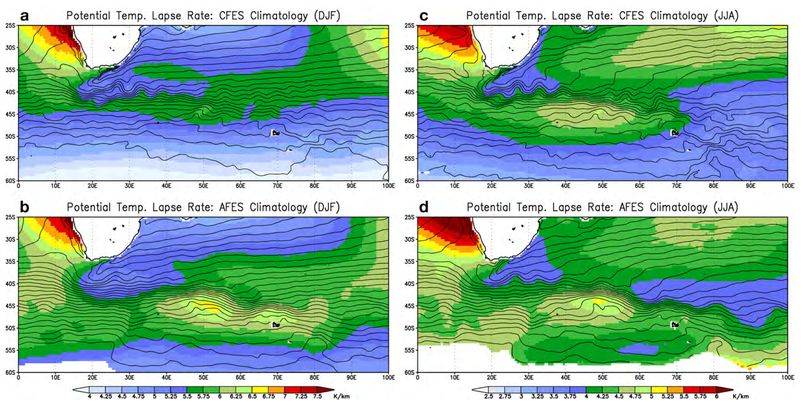

Figure 11. Climatology of potential temperature lapse rate [K km^{-1}], defined as the vertical gradient of potential temperature between 700 and 1000 hPa, calculated from (top) CFES and (bottom) AFES for (left) DJF and (right) JJA. Note that color bars are different between DJF and JJA.

Acknowledgements

This study is partially supported by Grant-in-Aid for Scientific Research on Innovative Area **'Multi-scale air–sea interaction under the East-Asian monsoon: A "hot spot" in the climate system'** and so on. The numerical calculation was carried out on the Earth Simulator under support of JAMSTEC.